Title Poly(ethylene oxide)-*b*-poly(l-lactide) Diblock Copolymer/Carbon Nanotube-Based Nanocomposites: LiCl as Supramolecular Structure-Directing Agent

Authors Franck Meyer, Jean-Marie Raquez, Pierre Verge, Inger Martínez de Arenaza, Borja Coto, Pascal Van Der Voort, Emilio Meaurio, Bart Dervaux, Jose-Ramon Sarasua, Filip Du Prez, and Philippe Dubois

In: Journal, Volume (Issue), pages, year. Biomacromolecules, 12 (11), 4086-4094, 2011

Optional:

Poly(ethylene oxide)-*b*-poly(L-lactide) diblock copolymer/carbon nanotube-based nanocomposites: fine-tuning of materials morphology mediated by LiCl as supramolecular structure-directing agent.

Franck Meyer,[*†] *Jean-Marie Raquez,*[†] *Pierre Verge,*[†] *Inger Martínez de Arenaza,*[§] *Borja Coto,*[‡] *Pascal Van Der Voort,*[◊] *Emilio Meaurio,*[§] *Bart Dervaux,*[†,#] *Jose-Ramon Sarasua,*[§] *Filip Du Prez,*[#] *Philippe Dubois**[†]

†Laboratory of Polymeric and Composite Materials, Center of Innovation and Research in Materials and Polymers (CIRMAP), University of Mons UMONS, Place du Parc 20, 7000 Mons, Belgium, §Department of Mining-Metallurgy and Materials Science School of Engineering, University of the Basque Country (EHU-UPV) Alameda de Urquijo s/n. 48013 Bilbao, Spain, ‡Fundacion Tekniker, Avda Otaola 20, 20600 Eibar, Spain, ◊Centre for Ordered Materials, Organometallics and Catalysis (COMOC), Department of Inorganic and Physical Chemistry, Ghent University, Krijgslaan 281 S3, 9000 Gent, Belgium, #Polymer Chemistry Research Group, Department of Organic Chemistry, Ghent University, Krijgslaan 281 S4 bis, 9000 Gent, Belgium

* To whom correspondence should be addressed. E-mail: Franck.Meyer@umons.ac.be and Philippe.Dubois@umons.ac.be

[†]Laboratory of Polymeric and Composite Materials

ABSTRACT: This work relies on the CNT dispersion in either solution or a polymer matrix through the formation of a three component supramolecular system composed of PEO-*b*-PLLA diblock copolymer, carbon nanotubes (CNTs) and lithium chloride. According to a *one-pot* procedure in solution, the "self-assembly" concept has demonstrated its efficiency using suspension tests of CNTs. Characterizations of the supramolecular system by photon correlation spectroscopy, raman spectroscopy and molecular dynamics simulations highlight the charge transfer interaction from the CNTs towards the PEO-*b*-PLLA/LiCl complex. Finally, this concept was successfully extended in bulk (absence of solvent) via melt-processing techniques by dispersing these complexes in a poly(L-Lactide) (PLA) matrix. Electrical conductivity measurements and transmission electron microscopy attested for the remarkable dispersion of CNTs, leading to high-performance PLA-based materials.

KEYWORDS: carbon nanotubes, polylactide, poly(ethylene oxide), supramolecular interactions, reactive extrusion, nanocomposites, molecular dynamics simulations

Introduction

Over the last two decades, carbon nanotubes (CNTs) have attracted a special attention to design new nanocomposites due to a unique combination of mechanical, thermal, structural and electrical properties.[1-3] In the field of biotechnology, CNTs-based biomaterials have also proved quite versatile with applications as diverse as prosthesis, biomolecular recognition and drug delivery systems. [4] Nonetheless, strong intermolecular π-π interactions between the nanotube walls and their high aspect ratio lead to a bundle-like arrangement, which represents a major drawback for their processability and application. [5] Different strategies aiming at the dispersion of the CNTs in solution or in a polymer matrix have thus been developed. Most of them lie in the non-covalent and covalent functionalizations of CNT surface. [6] However, the supramolecular approach is emerging as a very appealing pathway since it takes advantage of the preservation of the unsaturated conjugated structure. [7-8] This is also supported by a wide range of non-covalent interactions, performed in a reliable and cost-effective manner. For instance, these

non-covalently coated CNTs maintain their intrinsic features, namely a robust mechanical behavior, a high electronic conductivity, and their potential biosensing properties.

Poly(ethylene oxide) (PEO) belongs to the class of polyethers, exhibiting good solubility in water and organic solvents. As far as their applications are concerned, PEO-containing compounds are used as excipients or as carriers in different biological materials, foods and cosmetics. Moreover, these polymers can develop a specific behavior under varied stimuli such as temperature and salt concentration. Another interesting feature of PEO lies in a specific property, which is closely related to the crown ethers, namely the high affinity of the ethyleneoxy segments for various cations. [9] In the presence of an inorganic salt, oxygen atoms belonging to the polymeric chain coordinate the cation, locating it in the middle of a loop. This creates a separation of charge (cation-anion) and leads to the formation of "super" cationic species with an expected high affinity for the CNT surface. [10] For instance, we have recently demonstrated that poly(*N*-(2-(dimethylamino) ethyl)-methacrylate (PDMAEMA) is capable of maintaining a stable CNT dispersion in acidic media (as polyelectrolyte). [11-12] In the same way, a poly(L-lactide) (PLLA) ω-functionalized with an imidazolium moiety endowed a high binding ability towards the π-conjugated surface thanks to cation-π interactions. [13-14]

In this work, we decided to develop an original approach relying on the self-assembly of PEO-*b*-PLLA diblock copolymers, lithium chloride (LiCl) and CNTs according to a *one-pot* procedure. Consequently, we assumed that the association of a PEO segment with a PLLA block in the presence of an inorganic salt could give rise to a new biocompatible system with a high CNT dispersing ability in organic media (Figure 1).

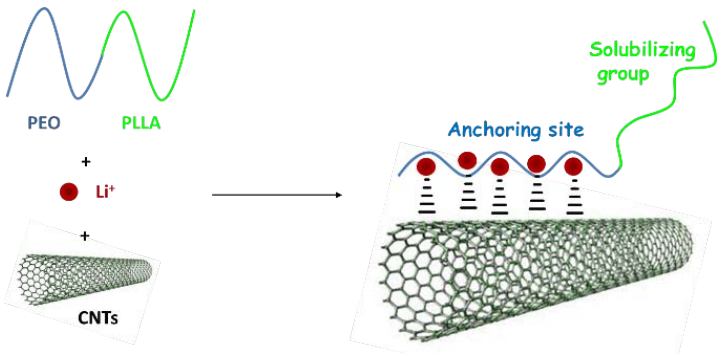

Figure 1. Concept of CNT dispersion with a PEO-*b*-PLLA/LiCl complex

The PEO/salt part[15] is selected to interact strongly with the CNT surface, while the PLLA is selected to confer a good solubility in an organic solvent and, subsequently, a good compatibility within a PLA matrix. First, the diblock copolymers were readily obtained by ring-opening polymerization of L-lactide initiated from a monohydroxylated PEO macroinitiator,[16] followed by a dispersion test of CNTs in solution. Photon correlation spectroscopy (PCS), Raman spectroscopy and force field-based molecular modeling enabled to provide key-information related to the behavior of the PEO-*b*-PLLA/LiCl complex in solution as well as the nature of interactions. Finally, the preparation of CNT-based nanocomposites was extended by reactive extrusion using the PEO-*b*-PLLA/LiCl complex as dispersing agent in a PLA matrix. The CNT dispersion was straightforwardly evaluated by comparison of the electrical percolation threshold of the final PLA/PEO-*b*-PLLA/LiCl/CNTs compound with respect to PLA/PEO-*b*-PLLA/CNTs samples and correlated with transmission electron microscopy.

Experimental section

Materials

The multi-wall carbon nanotubes (MWCNTs, NanocylTM NC 7000) were supplied by Nanocyl S.A. (Belgium). These MWCNTs were produced via a catalytic carbon vapour deposition (CCVD) process. L-lactide was supplied by Purac (The Netherlands) and recrystallized from dry toluene. Toluene, THF and chloroform were purchased from VWR and distilled before use. 1,8-diazabicyclo[5,4,0]undec-7-ene (DBU) as metal-free catalyst was purchased from Aldrich and distilled over barium oxide before use.

Acetic acid and hexane were purchased from ChemLab. LiCl was purchased from Acros. Poly(ethylene glycol) monomethyl ether (M_n= 2000 and 5000 g/mol) with a polydispersity index (M_w/M_n) of 1.05 was purchased from Fluka chemika. Commercial poly(L-lactide) (PLLA) was industrially produced by NatureWorks (U.S.) (NatureWorks® PLLA Polymer 4032D); PLLA was characterized by a number average molecular weight of 130 Kg mol^{-1} (PS standards), a polydispersity index of 1.9, and a D-isomer content estimated to 4.4 wt%.

Characterization

Size-exclusion chromatography (SEC) was performed in chloroform at 35°C using a Polymer Laboratories liquid chromatograph equipped with a PL-DG802 degasser, an isocratic HPLC pump LC 1120 (flow rate = 1 mL/min), a Marathon autosampler (loop volume = 200 μL, solution conc. = 1 mg/mL), a PL DRI refractive index detector and three columns: a PL gel 10 μm guard column and two PL gel Mixed-B 10 μm columns. Polystyrene standards were used for calibration. Sample weight was generally in the range of 5 to 10 mg. ^{1}H NMR spectra were recorded on a 500 MHz nuclear magnetic resonance spectrometer (Bruker AVANCE 500). PCS was operated with a Malvern zetasizer nano zs. Raman measurements were performed on a Kaiser Raman RXN optical system using IC Raman 4.1 software, equipped with an Invictus™ solid state diode-pumped 532nm Laser (100mW power). The electrical conductivity measurements were carried out following two different methods to record the evolution of the resistivity as a function of the CNT content since each apparatus is not able to scan the full resistivity range. Resistivity of the nanocomposites is highly affected by the CNT content and varies in a broad range. For moderately conductive materials (resistance below 10^8 Ω), a two-probe test method was used, with an apparatus composed of a Keithley 2750 multimeter, a two-probe measurement device and two pairs of grips. The electrical measurement principle consists of submitting an electrical current to rectangular bars of 1.2 x 8 x 0.3 cm^3 and to determine the value of the induced voltage. The electrical resistance is directly supplied by the multimeter. For surface resistance measurements, silver paint was coated on the extremities of a bar with a length of about 0.5 cm: this small area is the contact between

the electrodes and the samples. Using the two grips (coated with copper sheet) between the two silver coated areas, the value of the resistance (R) between the two painted parts was measured. The surface resistivity (ρ) is then calculated following the formula: R.L/l=ρ where l and L are respectively the distance between the two coated areas and their width. The result is expressed in Ω/❑ (ohm per square). Samples (diameter : 100 mm; thickness : 0.5 mm) were prepared from the extruded material by compression molding at 175°C, with a pre-heating step of 1 min, a heating step of 5 min under a pressure of 200 bar and a cooling step with a pressure of 150 bar. Samples were then prepared as stripes (~30x10 mm^2), cut from the plates using a stamper. For insulating materials (resistance range: $10^8 \div 10^{18}$ Ω), an apparatus consisting of a 8009 Resistivity Text Fixture box combined with a 6517B Keithley electrometer was used. The electrical measurement principle consists of submitting a variable voltage to a specimen of 9x10 cm^2 surface and 3mm thick and to determine the value of electric current through it. In this case, the resistivity is determined through the plotting of V=f(I) for an accurate measurement. To obtain the disc shape, samples (diameter: 100 mm; thickness: 0.5 mm) prepared from the extruded material were compression-molded at 175°C, with a pre-heating step of 1 min, a heating step of 5 min under a pressure of 200 bar and a cooling step with a pressure of 150 bar. Samples were prepared from the extruded material, which was compression-molded into parallel compression molded plate (diameter of 25 mm and thickness of 10 mm) at 175°C, with a pre-heating step of 1 min, a heating step of 5 min under a pressure of 200 bar and a cooling step with a pressure of 150 bar.

Typical procedure for the synthesis of PEO-b-PLLA diblock copolymers ***1-6***

L-lactide (17.5 g, 121.5 mmol) and poly(ethylene glycol) monomethyl ether (6.94 g, 3.47 mmol) were stirred in chloroform (61 mL). DBU (128 µl, 0.87 mmol) was added and the solution was stirred at room temperature for 10 min. Then, three drops of acetic acid were added and the resulting mixture was precipitated in heptane. After filtration, the white powder was dried at 70 °C under vacuum overnight. Yield = 95%. M_n determined by SEC in $CHCl_3$ = 10000 g/mol^{-1}, PDI = 1.09.

Typical procedure for the preparation of MWCNTs dispersion with PEO-b-PLLA diblock copolymers ***1-6***

100 mg of PEO-*b*-PLLA diblock copolymers **1-6**, 5 mg of MWCNTs and 100 µL of LiCl sat. are stirred in THF (10 mL) overnight. Then, the mixture was centrifugated at 4000 rpm for 10 mn.

Typical procedure for the masterbatch preparation

0.45 g of MWCNTs, 1.5 g PEO-*b*-PLLA diblock copolymer **2**, 0.9 ml of LiCl sat. are stirred in THF (60 mL) for 5h. After evaporation of the solvent, the residue and 1.05 g of PLA 4032D are stirred in chloroform (60 mL) for 5h. The solvent was subsequently evaporated under reduced pressure at 60°C in order to recover the corresponding masterbatches. For PLLA/PEO-*b*-PLLA/CNTs and PLLA/CNTs/PEO-*b*-PLLA/LiCl samples, the amount of nanotubes was in the range from 0.5 to 25 wt% and the amount of PEO-*b*-PLLA was fixed at 50 wt% of the overall masterbatch amount.

Simulation details and computational specifications

The simulation process was performed with Materials Studio Modelling (Version 4.1) installed on Centos 5, obtained from Accelrys, USA. The present systems was generated using Discover and Amorphous Cell program, which is based on the combined use of the arc algorithm by Theodorou and Suter and the scanning method of Meirovitch.[17-18]

This study includes the construction of representative amorphous cells, consisting on (co)polymer chains, (6,6) single-wall CNTs (SWCNTs) and LiCl salt molecules. Initially, concentrated tetrahydrofuran (THF) solutions (around 10 wt %) were modelled. As these systems were extremely complex because of the large number of different components and the large number of molecules, THF was removed from the systems to simplify the analysis. The amorphous cells, summarized in Table 1, were accordingly constructed. The first one contains PEO-*b*-PLA chains, and LiCl salt molecules. The second one also contains SWCNTs and LiCl in the same quantities, but the PEO-*b*-PLLA copolymer is

replaced by poly(ethylene oxide) in order to gain insight about the effect of PLLA on the improvement of the SWCNTs dispersion.

Table 1. Composition of the amorphous cells.

Cell id. #	Composition of the simulation cell.	PEO repeat units	PLLA repeat units	Polymer chains	LiCl molecules	SWCNTs
1	PEO-*b*-PLA/ LiCl/SWCNTs	5	5	20	10	10
2	PEO/LiCl/SWCNTs	10	-	20	10	10

The amorphous cells were minimized for proper filling increasing the number of contacts between molecules. After minimization, all the systems were refined by molecular dynamics calculations. The systems were equilibrated for 5 ps at 298K, with time step of 1fs in the NPT ensemble (constant number of particles, pressure, and temperature). Pressure was fixed at 1atm using the Andersen method,[19] which allowed the cell volume to change with the pressure and temperature. Periodic boundary conditions were applied in all three spatial directions. The COMPASS (Condensed-phase Optimized Molecular Potentials for Atomistic Simulation Studies) forcefield[20] was used in this research. Electrostatic energies were calculated using the Ewald summation method, highly accurate in the calculation of long range interactions. An accuracy of 0.001 kcal/mol with an update width of 3Å was applied to evaluate electrostatic interactions.

Results and discussion

Synthesis of PEO-b-PLLA diblock copolymers

A series of PEO- *b*-PLLA diblock copolymers were prepared by ring-opening polymerization of lactide initiated from a fixed PEO chain length of 2000 or 5000 g/mol in chloroform at room temperature (Table 2). In contrast to the commonly used tin(II) octoate as catalyst, [21-24] 1,8-diazobicyclo[5.4.0] undec-7-ene (DBU) was used as a metal-free catalyst (Figure 2) since our target

consists in the formation of harmfulless biomaterials. The reactions were carried out with a DBU/alcohol initiator ratio of 0.25/1.

Figure 2. Synthesis of PEO-*b*-PLLA diblock copolymers by ROP of L-lactide.

Molecular characterizations of PEO-*b*-PLLA diblock polymers **1-6** were monitored through the relative number-average molecular weight (M_n) and associated polydispersity indices (PDI) as determined by gel permeation chromatography (GPC), and by ^{1}H NMR spectroscopy.

Table 2. Molecular characterizations of PEO-*b*-PLLA diblock copolymers

copolymer	PEO block (g/mol)	PLLA block (g/mol)		PDI[b]
		Th	Exp[a]	
1	2000	4000	4000	1.06
2		10000	10000	1.09
3		20000	20400	1.11
4	5000	5000	5200	1.04
5		10000	9800	1.05
6		20000	19200	1.6

[a]: determined by ^{1}H NMR

[b]: determined by GPC

In all cases, the ^{1}H NMR spectra revealed a good correlation between theoretical and experimental number-average molecular weights, i.e. PLLA chain lengths of ca. 4000, 10000 and 20000 g/mol from PEO of 2000 g/mol, and PLLA segments of ca. 5000, 10000 and 20000 g/mol with a PEO of 5000 g/mol. Moreover, the narrow PDIs of compounds **1-5** were in the range 1.04 to 1.11, confirming a good control over the reactions (Table 2). However, the diblock copolymer **6** exhibited a definitely higher PDI

(1.6). Despite several attempts, we did not succeed in the decrease of the dispersity but investigations aiming at the optimization of this reaction are beyond the scope of this article.

CNTs dispersion tests

In order to explore the CNTs dispersion with the PEO-*b*-PLLA/LiCl systems, the inorganic salt was employed as a saturated solution in water, and tests were performed in THF due to its miscibility with water. LiCl was selected as inorganic salt due to its well known affinity to PEO-based segments.[25] Preliminary dispersion experiments were run with each partner to eliminate a possible bias (Figure 3). Accordingly, 100 mg of PEO (2000 and 5000 g/mol) were mixed with 5 mg of CNTs in 10 mL of THF. After overnight stirring at room temperature, the resulting solutions revealed a complete sedimentation of CNTs. In a second step, 100µL of LiCl picked from a satured aqueous solution in LiCl (LiCl sat.) was added to the previous mixtures but after several hours of vigorous stirring, the solutions remained colorless. We had already demonstrated that PLLA is not able to maintain a stable CNT dispersion without appropriate binding group.[13-14] In the present study, the same result was observed in the presence of 100 µL of LiCl sat. However, a mixture of PEO, PLLA and LiCl sat. could give rise to a system with a high affinity to the CNT surface by a self-assembly of the compounds. In this regard, a mixture of 50 mg of PEO (2000 g/mol), 50 mg of PLLA (10000 g/mol) and 100 µL of LiCl sat. was stirred in 10 mL of THF in the presence of 5 mg of CNTs. Again, this test led to a complete and immediate sedimentation of CNTs. In contrast, a markedly different behavior was observed when the dispersion tests of CNTs were studied with diblock copolymers **1-6**. For instance, 100 mg of compounds **1-3** were stirred in the presence of 5 mg of CNTs and 100 µL of LiCl sat. in 10 mL of THF. After a few hours of vigorous stirring, the successive centrifugation has afforded deeply black solutions, stable over a period as long as two months, i.e., no trace of CNTs sedimentation was observed.

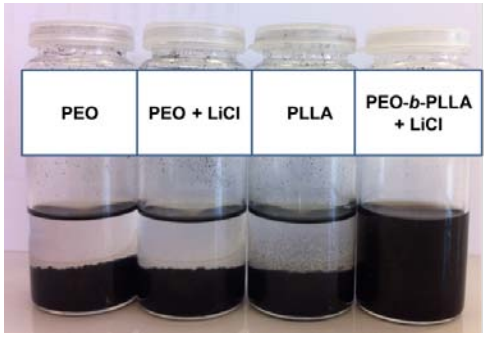

Figure 3. Dispersion of MWCNTs in THF in presence of PEO (5000 g/mol), PEO + 100 µL of LiCl sat., PLLA and PEO-*b*-PLLA **2** + 100 µL of LiCl sat.

Interestingly, these observations were achieved for diblock copolymers **1-3**. At this stage, we tried to determine the minimum amount of LiCl sat. necessary for a good and stable dispersion of CNTs. In all cases, highly black solutions were observed with a quantity of LiCl sat. down to 60µL; at lower content, solutions appeared colorless (Table 3). Proceeding with PEO-*b*-PLLA copolymers **4-6**, new mixtures composed of 100 mg of polymer, 5 mg of CNTs and 100 µL of LiCl sat. were prepared and stirred overnight in 10 mL of THF.

Table 3. minimum amount of LiCl sat. required for good CNT dispersion in THF with copolymers **1-6**

Copolymer PEO-*b*-PLLA (Mn_{PEO}-Mn_{PLLA})	LiCl sat. (volume)
1 (2000-4000)	60 µL (~1.2 mmol)
2(2000-10000)	
3 (2000-20400)	
4 (5000-5200)	40µL (~0.8 mmol)
5 (5000-9800)	
6 (5000-19200)	

After centrifugation, the exquisite character of the PEO-*b*-PLLA/LiCl supramolecular systems was again highlighted by a deeply black solution and the absence of sedimentation over a period of two months (no CNTs sedimentation was observed). Finally, subsequent experiments revealed that a

quantity of LiCl sat. higher than 40µL (0.8 mmol) is required for a good and stable dispersion of CNTs with compounds **4-6** (Table 3).

As aforementioned for PEO-*b*-PLLA **1-3**/LiCl mixtures, the minimum quantity of inorganic salt remains unchanged, independent of the PLLA block length.

PCS analysis

To address the issue of how PEO-*b*-PLLA **1-6** and LiCl interact, PEO-*b*-PLLA solutions were prepared with 100 mg of polymers **2** and **5** in 10 mL THF, and then mixed with varied quantities of LiCl sat., namely 10, 30, 60 and 100 µL. The solutions were characterized by photon correlation spectroscopy (PCS) (Table 4). From this results that the formation of monodisperse nanoobjects from diblock copolymers with an apparent hydrodynamic diameter ranging from 10 to 30 nm only occurs when 60 µL or more LiCl sat. is added to the PEO-*b*-PLLA diblock polymers **2** and **5**, i.e. when stable dispersions of CNT are formed.

Likewise, such behavior can be explained by the formation of ionic micelles via self-assembling/complexation formed between LiCl and PEO-block from PEO-*b*-PLLA diblock polymers. These micelles are more likely able to disperse CNTs in solution. It is worth noting that the apparent hydrodymanic diameter was independent of the quantities of LiCl sat. after adding 60µL in LiCl sat.

Table 4. average size of the micelles formed by diblock copolymers **2** and **5** in the presence of LiCl sat. as determined by PCS.

LiCl sat. (volume)	Average hydrodynamic diameter	
	PEO-*b*-PLLA **2**	PEO-*b*-PLLA **5**
10 µL	ND	ND
30 µL	ND	ND
60 µL	10-15 nm	10-15 nm
100 µL	10-15 nm	20-25 nm

ND: not detected

Raman analysis

Raman spectroscopy was also studied to elucidate the interaction between the PEO-*b*-PLLA **2**/LiCl complex and the CNTs. This spectroscopy represents a useful tool, frequently used for characterizing CNT-based materials. [26] All measurements were performed on a dispersive Raman instrument at an excitation wavelength of 532 nm. The region around 1580 cm^{-1} that is typical for the tangential vibration modes (also referred to as 'G' band) of CNTs, has been investigated. The Raman spectrum of the as-received CNT revealed a G band at 1572 cm^{-1} (Figure 4). In comparison, the PEO-*b*-PLLA 2/LiCl/CNT mixture exhibits a significant up-shift from 1572 to 1587 cm^{-1} for the G band. Such an up-shift can be explained by a charge transfer from the CNTs to the PEO-*b*-PLLA/LiCl system and is indicative of a strong interaction between both. For instance, a similar behavior has been described for CNTs that were dispersed in a nitrile functionalized polyimide matrix. [27]

Another important Raman signal for CNTs appears in the region 1200 – 1500 cm^{-1} (D band) and is associated with the extent of disorder and defects present along the nanotube. The intensity ratio between the D- and G-bands (I_D/I_G) can also correlate the dispersion quality of the CNTs. However, unlike the well-resolved G-band, it was difficult to identify the CNT D-band in the Raman spectrum of the PEO-*b*-PLLA **2**/LiCl/CNT system due to an overlap with the polymer signals (see Figure S1 in Supporting Information).

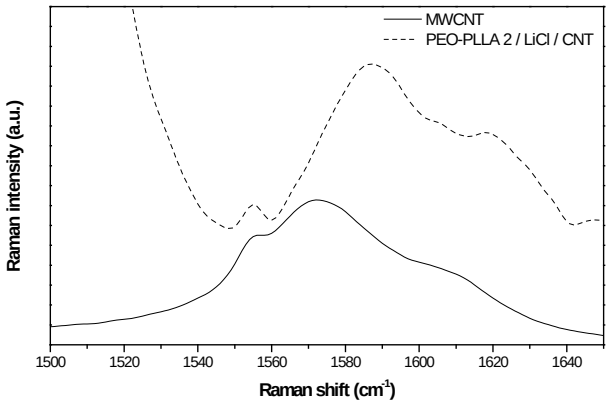

Figure 4. Raman spectra focusing on the tangential modes (G modes) of pure MWCNTs (—) and the PEO-*b*-PLLA **2**/LiCl/CNT system (- - -).

It is obvious that the ratio I_D/I_G is not increasing significantly, indicating that the amount of disorder/structural defects on the CNT is not increasing upon addition of the stabilizing polymer-salt system. Therefore, it can be deduced that no covalent bonds have been formed.

Molecular dynamics simulations of PEO-*b*-PLLA/CNT/LiCl and PEO/CNT/LiCl systems

In order to shed some light on the three component system (PEO-*b*-PLLA/CNT/LiCl), Molecular dynamics (MD) simulations have been carried out to analyze the mode of interaction occurring between single-walled carbon nanotubes (SWCNT)s used as model, lithium chloride and PEO homopolymer or the PEO-*b*-PLLA block copolymer. The analysis of the interactions in these systems may help to explain the dispersion of the CNTs in solution.

Before dealing with the analysis of the complete systems, the first step consisted in the determination of the nature of any possible interacting structures occurring within these systems. The behavior of the PEO-*b*-PLLA and PEO polymer chains in the presence of LiCl molecules is shown in Figure 5a. During the course of the MD simulations, the formation of crown ether-like structures in which the ethylene oxide segments surround the lithium cations is clearly observed, both in case of the homopolymer (PEO) or the copolymer (PEO-*b*-PLA) chains.

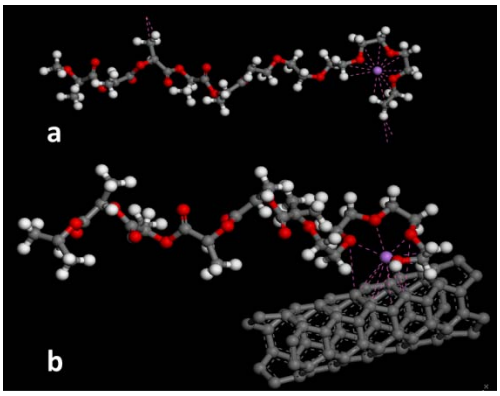

Figure 5. Snapshots showing: a) the formation of "crown ether"-cation complexes in a system containing Li^+ and PEO and b) simultaneous cation-"crown ether" and cation-π interactions in a system containing PEO-*b*-PLLA copolymer, Li^+ and SWCNT. Atom colours: gray: C; white: H; red: O; purple: Li^+.

The attractive force between the cation and the crown ethers is known to be purely electrostatic, through ion-dipole interactions, resulting in strongly bonded complexes.

In addition, approaching SWCNT to Li^+ ions results in the occurrence of cation-π interactions (see Figure 5b). Quite simply, these interactions are attributed to the electrostatic attraction between the positive charge of the cation and the regions of high π-electron density located above (and below) the rings of the SWCNT.

As can be seen in Figure 5b, the cation interacts with the center of the rings, but not with the edges (C-C bonds). Due to their strength, these interactions ought to be considered in the analysis of molecular conformations, such as protein structures, alongside with the more conventional hydrogen bonds, salt bridges, or hydrophobic effects. [28] The strong hydrophobicity of the CNTs and their autoassociating Van der Waals interactions usually result in the agglomeration of the CNTs. As discussed in the preceding paragraphs of this work, the presence of salt molecules in the system stimulates the formation of crown ether-like conformations, which promote the solubility of inorganic salts in organic solutions. In addition, the interactions between the Li^+ cations and the SWCNTs might also promote the dispersion of the nanotubes. Consequently, cells containing the three components (polymer, LiCl and the SWCNTs) have been modeled and are displayed in Figure 6 (see Table 1 for compositions).

The cells are automatically generated by the Amorphous Cell module using a proprietary algorithm. This system attempts to spread the different components across the whole volume, seeking at the same time for small energy configurations. Once generated, the cell is minimized to relax the input structure before running the MD simulations. The supramolecular system exhibits a high complexity, both in terms of the number of components and of the number of atoms. Therefore, taking into consideration the computational requirements of longer dynamics, determination of the global minimum through long MD simulations experiments seems unreasonable.

In spite of these limitations, the MD simulations can still provide some knowledge on the behavior of these systems. First, a qualitative description of the cells is made, as seen in Figure 6. The cell containing PEO (Figure 6a) shows CNTs poorly interacting with the polymer matrix (see for example

the two CNTs located on the top of the cell). This suggests that the local aggregation of CNTs should give rise to a hypothetical cell exhibiting a smaller energy than that in Figure 6a.

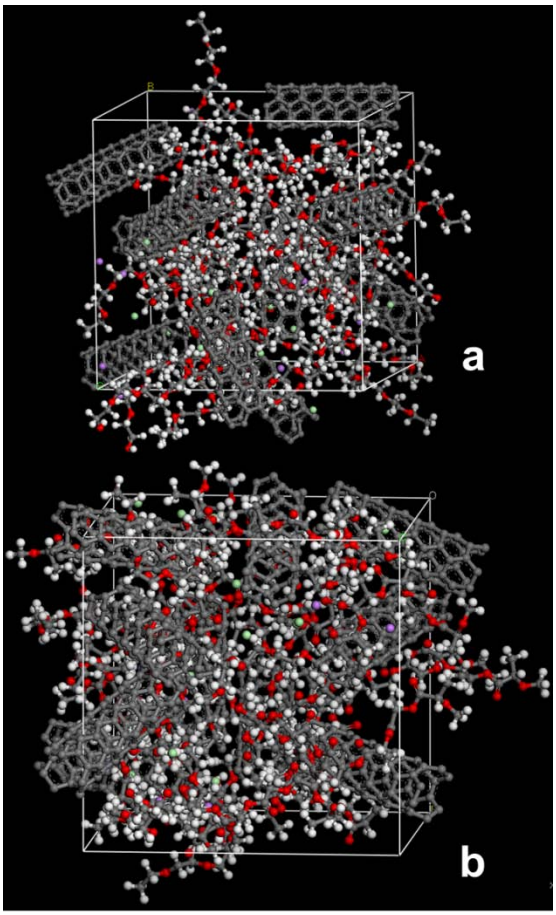

Figure 6. Snapshots of the cells after the MDs calculations in the NPT ensemble a) PEO/LiCl/SWCNT and b) PEO-*b*-PLLA/LiCl/SWCNT (see Table 1 for compositions). Atom colours: gray: C; white: H; red: O; purple: Li^+.

This observation is also supported by the favorable contribution corresponding to the π-π interactions between the CNTs. Therefore, the cell in Figure 6a highlights the favorable aggregation of the nanotubes with respect to their dispersion in this system. However, in case of the cell containing the PEO-*b*-PLLA copolymer (Figure 6b), all the CNTs show good contact with the polymer matrix (except, of course, the faces of the CNTs located in the outer limits of the cell, where all the contacts necessarily end).

These qualitative statements can be supported by calculating the energy of the interassociation interactions, E_{INT}, defined according to:

$$E_{INT} = E_T - E_{CNT} - E_{POLYMER} - E_{LiCl} \quad (1)$$

where E_T is the total energy and E_{CNT}, $E_{POLYMER}$ and E_{LiCl} are the energies calculated for each component, after removing all but the desired component from the cell obtained at the end of the MD simulation. For example, E_{CNT} is the energy calculated for the cell containing only 10 SWCNTs in the exact configuration obtained at the end of the MD simulations. The energy of the interassociation interactions, E_{INT}, reflects therefore the total strength of the interactions established between different components (not between different molecules of the same nature). Table 5 shows the values of E_{INT} for the cells of Figure 6. As expected, negative interaction energies have been obtained, indicating attractive interactions. However, the interactions are stronger for the cell containing the PEO-*b*-PLLA copolymer, in agreement with the qualitative analysis of the cells. For example, values above -311 kcal/mol for the cells containing aggregated CNTs would suggest that the system containing PEO prefers to lead to aggregated carbon nanotubes. In contrast the system containing PEO-*b*-PLLA prefers to yield individually dispersed CNTs.

Table 5. Detailed energy results obtained from the simulated amorphous cells.

Cell id. #	E_T (kcal/mol)	E_{CNT} (kcal/mol)	E_{PEO} (kcal/mol)	$E_{PEO\text{-}b\text{-}PLA}$ (kcal/mol)	E_{LiCl} (kcal/mol)	E_{INT} (kcal/mol)
1 (Figure 6a)	17290.00	26730.56	7.13	-	-9243.67	-204.00
2 (Figure 6b)	18216.56	26802.72	-	851.05	-9125.68	-311.52

In our opinion, the so-called "copolymer repulsion effect" could explain the better interactions between PEO segment and CNT observed in the system containing the PEO-*b*-PLLA copolymer.[29] In the system containing PEO only (Figure 6a), the polymer matrix seems to prefer the self-association of PEO chains over the establishment of interassociation interactions with CNTs. On the other hand, in the system containing the block copolymer, rejecting the CNTs would have resulted in unfavorable

interactions between dissimilar segments (polyethylene oxide-polylactide) covalently linked to each other. Hence, in the system containing PEO-*b*-PLLA, the unfavorable interactions of the PEO segments with PLLA seem to enforce an increase of the interactions between the PEO segments and the CNTs and to reject the PLLA segments in the solvent. Consequently, the number of contacts increases and renders PEO-*b*-PLLA copolymers able to disperse CNTs in this matrix.

Preparation of CNT-based compounds by reactive extrusion

The efficient CNT dispersion observed in the presence of PEO-*b*-PLLA/LiCl complex prompted us to study the dispersion of CNTs mediated with PEO-*b*-PLLA copolymers in a commercial PLLA matrix in bulk (absence of solvent) and at high temperature (ca. 185°C) via melt-processing techniques.

The PEO segment is used to get bound with lithium cations and create "super" cationic species with a high affinity binding for the π-conjugated surface, as previously evidenced in solution. As far as the PLLA chain is concerned, this polyester segment is used to confer a good miscibility of the PEO-*b*-PLLA/LiCl/CNT complex within the PLLA matrix and consequently to give rise to bio-based materials with finely dispersed CNTs during melt-processing. We should mention that we have demonstrated that imidazolium-functionalized PLLA chains as cationic species are able to interact with CNTs via cation-π interactions under the processing conditions used in this work.[13]

Keen to transpose the PEO-*b*-PLLA/LiCl/CNT supramolecular system to the preparation of CNT-based materials in bulk, these compounds were elaborated according to a two-step procedure, namely a masterbatch approach (for safety reason and easy handling), followed by the melt-blending of the resulting samples. Highly-enriched CNT masterbatches were produced first with PLLA, PEO-*b*-PLLA **2** in the presence (or not) of LiCl sat. For this, the polymer **2** was stirred in the presence of CNTs and LiCl sat. in THF, followed by the evaporation of the solvent under reduced pressure. Subsequently, the resulting samples were solubilized in chloroform and stirred with PLLA. The final compounds were characterized by an amount of CNTs ranging from 0.5 to 25 wt% and a fixed quantity of PEO-*b*-PLLA **2** of 50 wt% (Table 1S).

Table 6. Sample compositions after melt extrusion

Entry	Sample (CNTs wt %)	CNTs (wt %)	PEO-*b*-PLLA **2** (wt%)	PLA 4032 D (wt%)	LiCl sat. (ml)
1	PLLA/PEO-*b*-PLLA/LiCl	/	10	90	0.9
2	PLLA/ PEO-*b*-PLLA	/	10	90	/
3	PLLA/ PEO-*b*-PLLA /CNTs/LiCl 0.1%	0.1	10	89.9	0.9
4	PLLA/ PEO-*b*-PLLA /CNTs/LiCl 0.25%	0.25	10	89.75	0.9
5	PLLA/ PEO-*b*-PLLA /CNTs/LiCl 0.5%	0.5	10	89.5	0.9
6	PLLA/ PEO-*b*-PLLA /CNTs 0.5%	0.5	10	89.5	/
7	PLLA/ PEO-*b*-PLLA /CNTs/LiCl 0.75%	0.75	10	89.25	0.9
8	PLLA/ PEO-*b*-PLLA /CNTs 0.75%	0.75	10	89.25	/
9	PLLA/ PEO-*b*-PLLA /CNTs/LiCl 1%	1	10	89	0.9
10	PLLA/ PEO-*b*-PLLA /CNTs 1%	1	10	89	/
11	PLLA/ PEO-*b*-PLLA /CNTs/LiCl 2%	2	10	88	0.9
12	PLLA/ PEO-*b*-PLLA /CNTs 2%	2	10	88	/
13	PLLA/ PEO-*b*-PLLA /CNTs/LiCl 3%	3	10	87	0.9
14	PLLA/ PEO-*b*-PLLA /CNTs 3%	3	10	87	/

In a second step, the highly-enriched CNTs compounds were diluted by melt-blending with PLLA using a DSM vertical twin-screw extruder at ca. 185°C, with a screw rotation speed of 100 rpm and cycle time before flush of 5 min. These experiments gave a set of CNT-based materials with a CNT content ranging 0.1 to 3 wt%, and a fixed amount of PEO-*b*-PLLA **2**, namely 10 wt% (Table 6).

Determination of the electrical percolation threshold

The ability of the PEO-*b*-PLLA/LiCl complex as CNTs dispersing system was investigated through the determination of the electrical percolation threshold p_c. Indeed, it is well-established that better nanofiller dispersion leads to a threshold recorded at lower content of CNTs. Reciprocally, if a decrease

of p_c is observed, a better dispersion state of the nanofiller can be inferred. As depicted in Figure 7, the incorporation of the salt does not affect the electrical properties of the PEO-*b*-PLLA/PLA system, the resistivity remaining in the order of 5.10^{15} ohm.cm (entries 1-2, Table 6). Nevertheless, a clear trend appears when LiCl is combined with CNTs. Lower resistivities are reached at lower carbon nanotube content, evidencing that a better dispersion is reached when LiCl is employed (entries 3-14, Table 6).

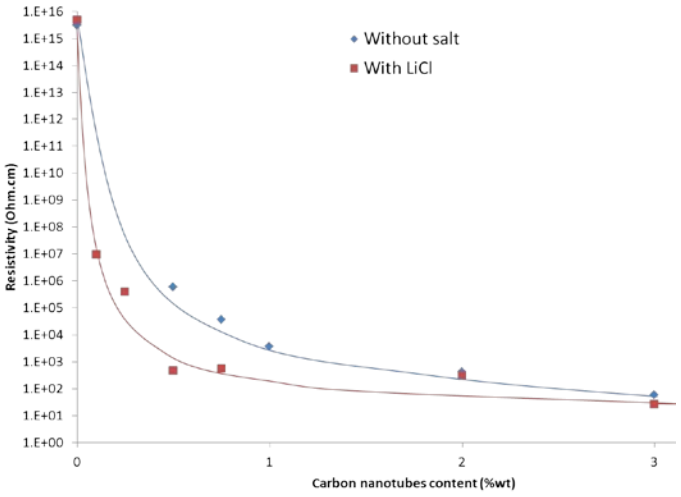

Figure 7. Evolution of the surface resistivity by increasing the CNT content for PEO-*b*-PLLA/PLLA/CNT nanocomposites prepared with or without LiCl (the lines are drawn to guide eyes only, and do not represent percolation curves).

Statistical percolation theory was then applied to determine accurately the percolation threshold of the two investigated systems. The electrical conductivity (σ) of the composites can be related to the volume fraction of the filler by the scaling law of the form:[30]

$$\sigma \alpha (V - V_c)^t \text{ for } V > V_c$$

where V is the volume fraction of fillers, V_c is the critical volume fraction, corresponding to the percolation threshold, and t is the critical exponent of conductivity that governs the scaling behavior in the region of Vc. If polymer and filler densities are almost equal, as in the case of PEO-*b*-PLLA and carbon nanotubes, the volume fraction can be replaced by weight fraction p and the previous equation becomes in logarithm:

$\log(\sigma(S/m)) \alpha\ t*\log(p-p_c)$ for $p>p_c$

The percolation threshold is obtained by plotting log(σ) versus log(p-p_c). p_c is obtained when the dots are aligned, i.e., for the highest correlation coefficient R^2 (Figure 8).

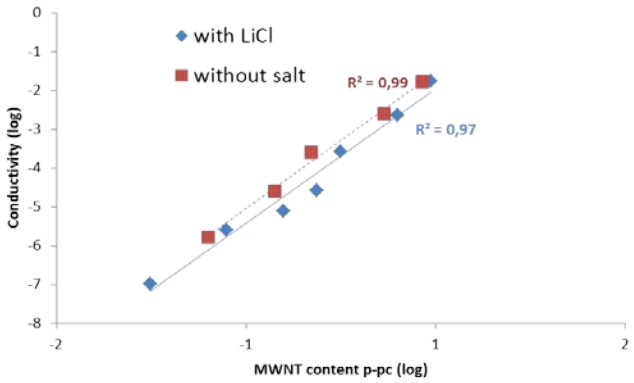

Figure 8. Logarithmic relationship between surface conductivity and CNT content in the absence and the presence of LiCl (linear fit for the determination of the percolation threshold).

For the CNT-based nanocomposites prepared in the presence of LiCl, the best fit is obtained for p_c tending to 10^{-3} wt%. In absence of salt, the percolation threshold is reached at only 0.3wt%. The decrease of the percolation threshold from 0.3 to 10^{-3} wt% owing to the presence of LiCl is an additional evidence for its dispersing ability.

TEM image analysis

This was confirmed for the nanocomposites containing 3wt% CNTs (entries 13 and 14, Table 6) using transmission electron microscopy (TEM). In the absence of LiCl, large CNT bundles together with some individual CNTs are observed (Figure 9a). In contrast, CNTs are mostly disentangled and fully dispersed/distributed throughout the matrix in the presence of LiCl (Figure 9b).

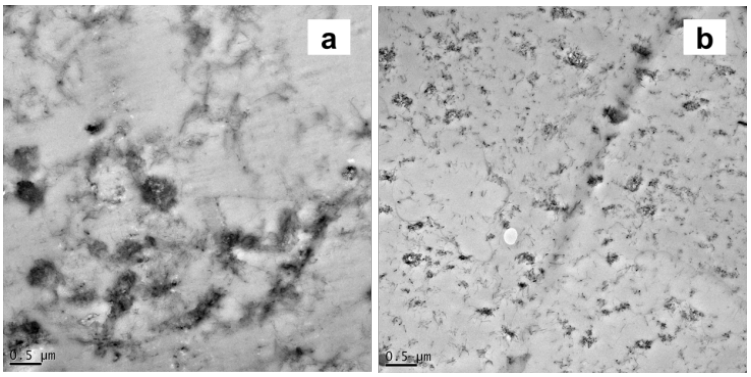

Figure 9. TEM images of PLLA/PEO-*b*-PLLA/CNT (3 wt% in nanotubes) nanocomposites (a) in the absence and (b) in the presence of LiCl.

Conclusions

In summary, we report the CNT dispersion in solution and in bulk on the basis of the self-assembly of a three-component system comprised of a PEO-b-PLLA diblock copolymer, LiCl and CNTs following a one-pot procedure. The concept relies upon the creation of "super" cationic species with high affinity with the CNT surface through chelation of lithium cations by the PEO segments. As far as the PLLA segment is concerned, it provides a good dispersion ability to the PEO-b-PLLA/LiCl/CNT supramolecular complex both in solution and in bulk.

Purposely, the synthesis of diblock copolymers was performed by ring opening polymerization of L-lactide initiated from ω-OH PEO macroinitiators. These diblock copolymers were recovered in good yields with good control over their molecular parameters. Subsequently, the CNT dispersion ability of the PEO-b-PLLA/LiCl complex was evaluated in THF with respect to pure starting materials. A dramatic variation of behavior was observed when the different species were challenged with the CNTs. Indeed, a complete CNT sedimentation was obtained when PEO, PEO/LiCl, PLLA and PLLA/LiCl were individually used as potential CNT dispersing agents. In contrast, PEO-b-PLLA/LiCl complexes have shown a high affinity with the π-conjugated surface owing to the large quantity of solubilized CNTs.

A second part of this work has dealt with the characterization of the mode of interaction between the PEO-b-PLLA/LiCl system and the CNTs. Thus, a PCS analysis highlights a good correlation between

the formation of micellar organizations and the minimum amount of LiCl content required for a good CNT dispersion. This was corroborated with various polymer chain lengths. Moreover, the CNT-based supramolecular materials were studied by Raman spectroscopy. Focusing on tangential vibration modes assigned to the CNTs, a significant up-shift from 1572 to 1587 cm-1 was evidenced for the G band, in agreement with a charge transfer from the electron-rich CNT surface toward the “super” cationic species (PEO-b-PLLA/LiCl). In order to shed some light on the complexation, Molecular Dynamics simulations were run. This results in a clear interaction between the cation-ethylene oxide segments and the CNTs driven by the self-assembly of the PEO-b-PLLA/LiCl/CNT partners. Moreover, further measurements gave a clear confirmation regarding a better CNTs dispersion with the PEO-b-PLLA/LiCl moieties with respect to PEO/LiCl. Finally, the concept was extended in bulk using a PLLA matrix. For this, samples were produced according to a two-step procedure (a masterbatch preparation followed by melt-extrusion), and the CNT dispersion was evaluated through the variation of electrical percolation threshold between samples with and without LiCl and by TEM images. The impressive “proof of concept” of this approach is thereby provided by a dramatic decrease of percolation threshold from 0.3 to 10-3 wt%, consistent with finely dispersed CNTs within the polyester matrix. In addition, TEM images supported the electrical conductivity analysis, showing a high CNT dispersion in the matrix as a clear and unambiguous proof of efficiency. Thus, this supramolecular strategy affords a reliable, rational and very efficient pathway for the CNT dispersion, both in organic media and in a polymer matrix. Such a concept can thereby be transposed to the formation of CNT-based nanocomposites with high-performance properties.

ACKNOWLEDGMENT

The research leading to these results has received funding from the European Community's Seventh Framework Programme FP7/2007-2013 under grant agreement n° 213939 (POCO project). Authors would like to thank the F.R.S.-FNRS for financial support. CIRMAP is very grateful to “Région Wallonne” and European Union (FEDER, FSE) for general financial support in the frame of Objectif 1-

Hainaut: Materia Nova, as well as to the Belgian Federal Government Office of Science Policy (SSTC-PAI 6/27). J-M. Raquez is “Chargé de recherche” within the Belgian F.R.S-FNRS. We want to thank A. Delafontaine for his technical support.

Supporting Information. Masterbatch compositions and RAMAN spectra “This material is available free of charge via the Internet at http://pubs.acs.org.”

REFERENCES

(1) Hirsch, A. *Angew. Chem. Int. Ed.* **2002**, *41*, 1853-1859.

(2) Niyogi, S.; Hamon, M. A.; Hu, H.; Zhao, B.; Bhowmik, P.; Sen, R.; Itkis, M. E.; Haddon, R. C. *Acc. Chem. Res.* **2002**, *35*, 1105-1113.

(3) Peng, X.; Wong, S. S. *Adv. Mater.* **2009**, *21*, 625-642.

(4) Polizu, S.; Savadogo, O.; Poulin, P.; Yahia, L. *J. Nanosci. Nanotechnol.* **2006**, *6*, 1883-1904.

(5) Spitalsky, Z.; Tasis, D.; Papagelis, K.; Galiotis, C. *Prog. Polym. Sci.* **2010**, *35*, 357-401.

(6) Karousis, N.; Tagmatarchis, N.; Tasis, D. *Chem. Rev.* **2010**, *110*, 5366-5397.

(7) Zhao, Y.-L.; Stoddart, J. F. *Acc. Chem. Res.* **2009**, *42*, 1161-1171.

(8) Lee, Y.; Geckeler, K. E. *Adv. Mater.* **2010**, *22*, 4076-4083.

(9) Ren, C.; Tian, W.; Szleifer, I.; Ma, Y. *Macromolecules* **2011**, *44*, 1719-1727.

(10) Pedersen, C. J. *J. Am. Chem. Soc.* **1967**, *89*, 7017-7036.

(11) Meyer, F.; Minoia, A.; Raquez, J.-M.; Spasova, M.; Lazzaroni, R.; Dubois, P. *J. Mat. Chem.* **2010**, *20*, 6873-6880.

(12) Olivier, A.; Meyer, F.; Desbief, S.; Verge, P.; Raquez, J.-M.; Lazzaroni, R.; Damman, P.; Dubois, P. *Chem. Commun.* **2011**, *47*, 1163-1165.

(13) Manfredi, E.; Meyer, F.; Verge, P.; Raquez, J.-M.; Thomassin, J.-M.; Alexandre, M.; Dervaux, B.; DuPrez, F.; Van Der Voort, P.; Jérôme, C.; Dubois, P. *J. Mat. Chem.* DOI:10.1039/C1JM12250A.

(14) Meyer, F.; Raquez, J.-M.; Coulembier, O.; De Winter, J.; Gerbaux, P.; P. Dubois, P. *Chem. Commun.* **2010**, *46*, 5527-5529.

(15) Chatterjee, T.; Yurekli, K.; Hadjiev V. G.; Krishnamoorti, R. *Adv. Func. Mater.* **2005**, *15*, 1832-1838.

(16) Coulembier, O.; Degée, P.; Hedrick, J. L.; Dubois, P. *Prog. Polym. Sci*. **2006**, *31*, 723–747.

(17) Theodorou, D. N.; Suter, U. W. *Macromolecules* **1985**, *18*, 1467-1478.

(18) Meirovitch, H. *J. Chem. Phys.* **1983**, *79*, 502-508.

(19) Andersen, H. C. *J. Chem. Phys.* **1980**, *72*, 2384–2393.

(20) Sun, H. *J. Phys. Chem. B* **1998**, *102*, 7338-64.

(21) Popelka, S.; Machová, L.; Rypácek, F. *J. Colloid. Interf. Sci.* **2007**, *308*, 291-299.

(22) Buwalda, S. J.; Dijkstra, P. J.; Feijen, J. *J. Control. Release* **2010**, *148*, e21-e56.

(23) Buwalda, S. J.; Dijkstra, P. J.; Calucci, L.; Forte, C.; Feijen, J. *Biomacromolecules* **2010**, *11*, 224-232.

(24) Wei, Q.; Li, T.; Wang, G.; Li, H.; Qian, Z.; Yang, M. *Biomaterials* **2010**, *31*, 7332-7339.

(25) Gray, F. M. Polymer electrolytes. *UK: The Royal Society of Chemistry*, **1997**.

(26) Lefrant, S.; Baibarac, M.; Baltog, I. *J. Mat. Chem.* **2009**, *19*, 5690-5704.

(27) Wise, K. E. Park, C.; Siochi, E. J.; Harrison, J. S. *Chem. Phys. Lett.* **2004**, *391*, 207-211.

(28) Ma, J. C.; Dougherty, D. A. *Chem. Rev.* **1997**, *97*, 1303–1324.

(29) Paul, D. R.; Barlow, J. W. *Polymer* **1984**, *25*, 487-494.

(30) Benoit, J. M.; Corraze, B.; Chauvet, O. *Phys. Rev. B* **2002**, *65*, 241405.

Table of Contents

F. Meyer,* J.-M. Raquez, P. Verge, I. Martínez de Arenaza, B. Coto, P. Van Der Voort, E. Meaurio, B. Dervaux, J.-R. Sarasua, F. Du Prez, P. Dubois*

Poly(ethylene oxide)-*b*-poly(L-lactide) diblock copolymer/carbon nanotube-based nanocomposites: fine-tuning of materials morphology mediated by LiCl as supramolecular structure-directing agent.